Article

Octupolar Metastructures for a Highly Sensitive, Rapid and Reproducible Phage-based Detection of Bacterial pathogens by SERS

Massimo Rippa, Riccardo Castagna, Marianna Pannico, Pellegrino Musto, Giorgia Borriello, Rubina Paradiso, Giorgio Galiero, Sergio Bolletti Censi, Jun Zhou, Joseph Zyss, and Lucia Petti

ACS Sens., **Just Accepted Manuscript** • DOI: 10.1021/acssensors.7b00195 • Publication Date (Web): 09 Jun 2017

Octupolar Metastructures for a Highly Sensitive, Rapid and Reproducible Phage-based Detection of Bacterial pathogens by SERS

Massimo Rippa,^[+] Riccardo Castagna,^[+] Marianna Pannico,[§] Pellegrino Musto,[§] Giorgia Borriello,[⊥,^] Rubina Paradiso,[⊥] Giorgio Galiero,[⊥] Sergio Bolletti Censi,[ς] Jun Zhou,[♣,^] Joseph Zyss[♦,^] and Lucia Petti*[,^]

^Institute of Applied Sciences and Intelligent Systems "E. Caianiello" of CNR, 80072 Pozzuoli, Italy

[§] Institute for Polymers, Composites and Biomaterials of CNR, 80072 Pozzuoli, Italy.

[⊥]Zooprofilattico Institute of the South, 80055 Portici, Italy

[ς] Cosvitec Scarl, 80100 Naples, Italy

[♣]Institute of Photonics, Faculty of Science, Ningbo University, Ningbo 315211, China

[♦]Laboratoire de Photonique Quantique et Moléculaire, CNRS and Ecole Normale Paris-Saclay, 94230 Cachan, France

KEYWORDS: metastructures, Localized Surface Plasmon Resonance, Surface Enhanced Raman Scattering, pathogen bacteria detection, agro-food

ABSTRACT: The development of fast and ultrasensitive methods to detect bacterial pathogens at low concentrations is of high relevance towards human and animal health care and diagnostics. In this context, surface-enhanced Raman scattering (SERS) offers the promise of a simplified, rapid and high-sensitive detection of bio-molecular interactions with several advantages over previous assay methodologies. In this work, we have conceived reproducible SERS nanosensors based on tailored multilayer octupolar nanostructures which can combine high enhancement factor and remarkable molecular selectivity. We show that coating novel multilayer octupolar metastructures with proper self-assembled monolayer (SAM) and immobilized phages can provide label-free analysis of pathogenic bacteria via SERS leading to a giant increase in SERS enhancement. The strong relative intensity changes of about 2100% at the maximum scattered SERS wavelength, induced by the *Brucella* bacterium captured, demonstrate the performance advantages of the bacteriophage sensing scheme. We performed measurements at the single-cell level thus allowing fast identification in less than an hour without any demanding sample preparation process. Our results based on designing well-controlled octupolar coupling platforms open-up new opportunities towards the use of bacteriophages as recognition elements for the creation of SERS-based multifunctional biochips for rapid culture- and label-free detection of bacteria.

Major research efforts are currently focused on the development of efficient field-ready sensor devices for the detection of pathogenic bacteria.[1-6] The presence of pathogenic bacteria in food and drinking water poses a threat to public health and security. To deal with this issue, an early-warning surveillance system is needed towards early in-situ early detection of bacteria. In this context, detection of *Brucella*, at the origin of brucellosis, is very challenging, since currently applied techniques are time-demanding and lacking standardization.[7] Despite the low lethality of brucellosis, the pending threat of zoonosis remains an important public health worldwide problem. Thus, the availability of a method that allows early and reliable identification of possible *Brucella* isolates would be extremely useful for both clinical and epidemiological reasons.

Current research focuses on the development of biosensors combining the engineering of materials and interfaces allowing for the enhanced transduction efficiency.[8-26] Towards this purpose, a combination of conventional techniques based on biological markers with label-free approaches is chosen.[12-17] Label-free biosensors are an efficient tool for the development of diagnostic systems, such as the use of high sensitivity plasmonic devices resting on variations in the electromagnetic modal spectrum, while selectivity is ensured by the specificity of biodetection mechanisms occuring at the surface. By means of plasmonic nanostructures, it is possible to synthesize novel nanobiosensors characterized by selective responses

which, in turn, undergo significant frequency shifts in the presence of biological material. Recently, techniques based on vibrational spectroscopy have emerged as powerful tools for the molecular characterization of biospecies.21 In particular, Surface Enhanced Raman Spectroscopy (SERS) has gained increasing attention in view of its applications to the detection and identification of unknown analytes at extremely low concentrations thanks to the unique spectral fingerprints of molecular vibrations from single molecule scale to unicellular organisms.[18, 27-28] In SERS, it is of crucial importance to develop metal nanostructures that are able to produce high field enhancement with highly reproducible features.[19-24] Development of novel SERS substrates with tailored interface targeting specific plays a pivotal role in determining the spectrum profile and SERS enhancement magnitude, as well as their applications. Generally, complex metallic nanostructures with a high SERS activity can either be fabricated by top-down nanolithography techniques or by bottom-up self-assembly approaches.[24,25,26,29] However, only nanolithography tools such as electron beam lithography (EBL) can provide a tight control on nanoparticle shape and size and inter-particle separation which account for the strength of the electric-field enhancement and plasmonic wavelength resonance.

In parallel, development of biosensitive surfaces involves the construction of a layer that contains elements (organic linkers) active in biomolecular recognition, that are immobilized at the surface of the transducer and present appropriate anchoring functionality to pathogenic bacteria. In this context, bacteriophages (a group of viruses) that recognize and lyse target specific bacteria have recently gained much attention as recognition elements for biosensing purposes.[30-33] Bacteriophages are an important component for the detection and identification of bacterial pathogens as well as potentially excellent tools for diagnostics and therapeutics of bacterial diseases. In addition, particular advantages in the use of bacteriophages consist in the specificity of their interaction with specific target host cell. However, this level of specificity and selectivity also opens avenues for the development of specific pathogen detection technologies. Such use of phages for the creation of pathogenic sensing platforms has been reported by using quartz crystal microbalance (QCM), flow cytometry, and surface plasmon resonance (SPR) as transduction platforms based on physical adsorption for the attachment of the phages on the sensor surface.[34-35] Nevertheless, it has been reported that chemical attachment of the phages onto surface yields better coverage and thus significantly improves the performance of these sensors.[33]

Herein, we investigate novel multilayer meta-structures, the chemical attachment of bacteriophages onto such meta-surfaces using a self-assembled monolayer (SAM) method, and their SERS response before and after bacteriophage immobilization. In this work, we report on the conception of highly sensitive and reproducible SERS nanosensors based on a novel multilayer octupolar metastructure functionalized with bacteriophages chemically bound on a self-assembled monolayer (SAM) of 4-mercaptobenzoic acid (4-MbA), enabling SERS response to the specific and label-free detection of *Brucella* bacteria. We study the fabricated nanopatterns by using optical (dark field microscopy) and morphological (Scanning Electron Microscopy) imaging techniques, and by AFM. Immobilized phages to the nanosensors and phage-bacteria interaction are monitored by SERS analysis. The multilayer octupolar-SERS substrates show high average enhancement factors of more than 10^6 with very good signal uniformity, thus enabling label-free detection of immobilized bacteriophages at femto-molar concentration level and aqueous *Brucella* bacteria at single-cell level exhibiting a remarkable 8-fold and 21-fold increase of the signal, respectively.

EXPERIMENTAL SECTION

Fabrication of Multilayer octupolar metastructure via EBL. We used high-resolution Electron Beam Lithography to fabricate the metastructures (Raith 150 EBL system). In the cell, the side of the three big triangles is 200 nm and the side of the smaller inner triangle is 80 nm. The minimal inter-particle distance between two neighbouring cells is 25 nm. A 100 nm layer of ZEP 520A positive resist (solution composed of 11% methyl styrene and chloromethyl acrylate copolymer (solid) and 89% anisole (solvent)) is spin-coated on a 15 nm conductive ITO coated glass substrate, baked at 170° for 5 min (to remove the anisole) and exposed to a 10.2 pA electron beam with an area dose of 23.5 μC/cm^2. Nanotriangular holes are generated in the resist layer after development in a n-Amyl acetate solvent, then rinsed for 90 sec in 1:3 MIBK:IPA solution (Isopropyl alcohol) for 60 sec, followed by IPA rinse for 30 sec. Finally, the gold octupolar array is created by evaporating a 50 nm gold film to the ZEP surface by e-beam process (SISTEC CL-400C evaporator). The final results are 2D (300 μm × 300 μm) nanostructures with increasing edge-to-edge distances from 25 to 100 nm in a 2-layers (ZEP/Au) configuration. The fabrication process and the cross section of the substrate are schematically shown in Figure 1a-b.

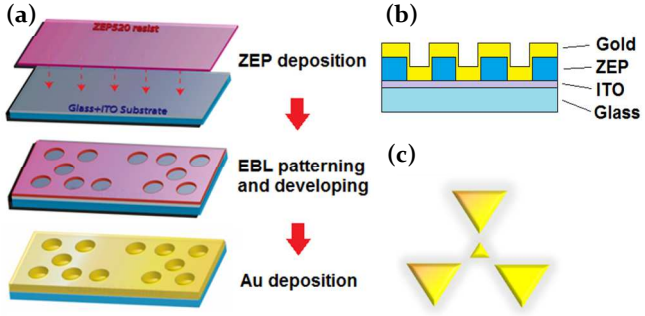

Figure 1. (a) Representation of the EBL process for multilayer nanostructure fabrication; (b) Scheme showing the cross section of the multilayer structure; (c) Meta-molecule design.

FDTD Simulation. Near field distributions were calculated using the finite difference in time domain (FDTD) method taking in account a computational domain corre-

sponding to an elementary cell of about 2x2 microns. Periodic boundary conditions along the x and z axes were used to simulate an infinite lattice based on the repetition of the elementary cell, while the Perfectly Matched Layer (PML) condition was considered for the y-axis to avoid the presence of spurious resonances in the solution. In the calculation, it was used a three dimensional spatial grid with step size of $\Delta x = \Delta z = \Delta y = 5$ nm while a time step of $\Delta t = 2 \times 10^{-3}$ μm (in units of cT) was set to respect the stability limit required for achieving stable and convergent numerical solutions. The refractive indices taken into account for the multilayer were $n_{air} = 1$, $n_{glass} = 1.51$, $n_{ito} = 1.79$, $n_{zep} = 1.55$ while the gold was modeled using the Drude parameters. The simulations were performed by exciting the grid with a Gaussian laser source that propagates along the y axis with a wavelength of 785 nm polarized in the plane of the nanoholes in the x direction (TE polarization). The Poynting vector distributions are calculated 25 nm above the plane of the nanoholes to avoid stair-stepped approximation error.

Propagation of Phage. *Tbilisi* bacteriophages (LGC Standards) were propagated on *Brucella* abortus using standard protocols. Brucella bacteria were cultured in Tryptic Soy Broth (TSB) at 37°C with 5% CO2. Phage enumeration and propagation was carried out by the double layer agar method.[36] Briefly, for phage propagation, 0.1 ml of an overnight bacterial culture was mixed to 5 ml of molten TSA soft (0.75% agar) and poured on a TSA plate. Single drops of 100 µl of viral suspension were spotted on the double layer plate and incubated at 37°C with 5% CO2. After overnight incubation, single plaques (4 plaques/ml) were mixed and resuspended in SM buffer (5.8 g NaCl, 2g of $MgSO_4 \cdot 7H_2O$, 50 ml of 1 M Tris-HCl pH 7.5 and 1 ml of 10% (v/v) gelatin in 1 L of distilled water), thoroughly vortexed and incubated at room temperature for 2h. After incubation, viral suspension was treated with chlorophorm (5% v/v) to kill bacterial cells, centrifuged at 10˙000 rpm × 10 min and the supernatant was filtered through 0.22 µm membranes and recovered for further propagation steps. After 5 consecutive cycles of propagation/chlorophorm treatment/filtration, bacteriophages were enumerated by plating serial dilutions on double layer agar plates and counting single lysis plaques. Viral suspension was finally concentrated to 10^8 PFU/ml and dialyzed against sterile MilliQ water by centrifugation at 2˙000 rpm × 30 min using tubes provided with a 100˙000 Da membrane (Sigma-Aldrich). All steps were carried out in a BSL3 facility.

Functionalization of Metastructures with Phages by Thiol-Chemistry. Once fabricated, the octupolar metastructures were functionalized with a Tbilisi bacteriophages suspension by use of 4-MbA SAM. 4-MBA_SAM, in turn, can chemically interact with target molecules. To obtain it, the nanostructures were immersed in a 4-MbA 100 µM solution for 5 h and then the sample was rinsed many times by Ethanol and deionized water. 4-MBA is widely used to form SAMs on gold substrates for SPR (or LSPR) sensors for many reasons: a) on the basis of its ability to be adsorbed on gold substrates, due to -SH groups present in its structure; b) it offers the possibility of further functionalizations due to carboxyl-group (in -para with respect to the -SH) on the aromatic ring of the molecule; c) furthermore, links of 4-MBA to proteins can be due to carboxyl-groups of 4-MBA and both the functional carboxyl-groups and the amino-groups of amino-acidic residues (e.g. such as those of Lysine). In this context, the proteic coating of the viruses (capsides) can be involved in non-covalent bonding with SAMs of 4-MBA.[37-38] Thus, successively, 300 µl of a bacteriophages suspension (10^7 PFU/ml) in water was dropped on the samples, and left at room temperature overnight, to allow for phage adsorption on the 4-MbA-functionalized surfaces. The samples were then washed many times by deionized water and dried by N2 flux. The 4-MbA SAM forms stable links with the bacteriophages onto the meta-surfaces, enabling SERS response before and after bacteriophage immobilization. The system is stable even at room temperature, since as mentioned, the measurements are performed after washing the sample many times by de-ionized water (H2Odd) and obtaining repeatable results. The long term stability is high (many months) if the sample is accurately stored in a dark room, at 4°C.

We used the bacteriophage *Tbilisi*, belonging to the family *Podoviridae* that specifically recognizes and lyses *Brucella abortus*. The *Tbilisi* phages are typically 70 nm in diameter with a 20 nm tail, and perform lytic cycles inside the host bacterium *Brucella abortus*. Prior to any optical or spectroscopic analysis, the bacteria were inactivated via formaldehyde treatment to ensure a higher working safety. Then, for *Brucella* analysis, 300 µl of bacterial suspension (10^5 CFU/ml) in water was dropped on the nanostructures functionalized with bacteriophages and maintained for 45 min until completion of the recognition process. The surfaces were rinsed with water and ethanol before SERS measurement so as to remove non-captured bacteria. At a second stage of the study, we worked with live *Brucella* cells in a laboratory of Bio-Safety Level 3 (BSL -3) using an optimized home-made prototypal portable Raman system.

Morphological and Optical characterization. Morphological characterization was realized by Scanning Electron Microscopy (SEM), Dark Field Microscopy (DFM) and Atomic Force Microscopy (AFM). SEM images (Raith 150 system) were analyzed using an acceleration voltage of 5KeV and a high efficiency secondary electron in-lens detector. In Figure 2 SEM images of the 2-layers photonic crystals are reported together with a simulation of their near-field properties.

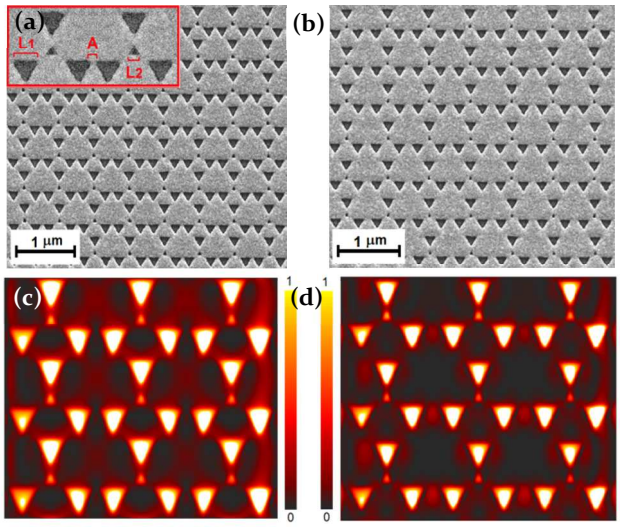

Figure 2. (a)-(b) SEM images of octupolar metastructures with L1=200nm, L2=70nm, A=25 nm and A= 100 minimum inter-hole distances between two neighbouring cells, respectively; c-d) calculated near field distribution for the octupolar nanostructures with L1=200nm, L2=70nm, A=25 (c) and 100 nm (d) minimum inter-holes distance between two near cells: Poynting vector distribution for the structures with minimum inter-hole gaps of 25nm and 100nm, respectively.

DFM images were obtained with white light illumination and the corresponding colorimetric fingerprints were collected by a 20X (N.A.=0.45) microscope objective. In Figure 3 DFM images of the octupolar nanostructures with inter-holes gap A=25nm are reported before and after phage deposition (a-b) together with a SEM image. The SEM image with virus was obtained after Au-palladium thin film deposition. In Figure 3c, bacteriophages are identifiable by their particular circular shape and white color. Their mean size was estimated of the order of 70 nm (Figure 3c, inset). Comparing the images obtained before (Figure 3a) and after (Figure 3b) bacteriophages immobilization, the color shift observed is due to the presence of viruses that induce a local refractive index change in the metallic film proximity. The uniformity of the color demonstrates the homogenous distribution of the viruses on the pattern.

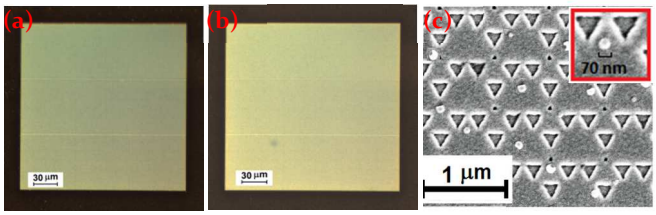

Figure 3. DFM images of the octupolar metastructure with A=25 nm before (a), and after (b) bacteriophages immobilization; c) SEM image after bacteriophages immobilization. The inset in (c) shows the metrology of a single phage.

AFM and topographic profiles measurements were collected with AFM-Ntegra Spectra, NT-MDT. AFM and topographic profiles measurements are also reported in the supporting information. SPR measurements were realized in transmission by using an Ocean Optics halogen white Lamp, an objective 40X, N. A. 0.65, and an Ocean Optics Spectrophotometer coupled to an optical fiber with core of 50 µm diameter to detect the signal.

SERS analysis. Mapping experiments were run by a confocal Raman spectrometer (Horiba-Jobin Yvon Mod. Labspec Aramis) operating with a diode laser source emitting at 785 nm. The 180° back-scattered radiation was collected by an Olympus metallurgical objective (MPlan 50×, NA = 0.75) with an exposure time of 1 s; a grating with 600 grooves/mm was used throughout. The radiation was focused onto a CCD detector (Synapse Mod. 354308) cooled at -70 °C by a Peltier module. In the mapping mode, a microscope slide containing the different SERS substrates was placed on a piezo-electrically driven microscope stage with a x,y resolution of 10 ± 0.5 nm and a z resolution of 15 ± 1 nm and scanned at a constant stage speed in the x-y plane with a 2.0 µm step size. The data gathered by the instrument were converted into ASCII format and transferred to the MATLAB computational platform for further processing. The SERS spectra were collected in the Raman-shift range 800–1800 cm^{-1}.
SERS analysis concerning the bacteriophages functionalization was performed by coupling the Raman system with an upright microscope Olympus BX51 in a backscattering configuration. The Raman system was QE Pro-Raman system (Ocean Optics), configured for λ = 785 nm (12 mW), with a grating of 1200 lines/mm and an input slit of 50 microns. The spectra were collected in the range between 400 - 2000 cm^{-1}, using 10 sec acquisition time of a 50x (N.A.= 0.75) microscope objective with an area of the spot size equals to 1.28 $µm^2$. In addition, the detection of live bacteria was realized in a laboratory of Bio-Safety Level 3 (BSL-3) coupling the spectrophotometer to a home-made prototypal system with more versatile features and more suitable for in-field analysis.

RESULTS AND DISCUSSION

Nanostructures Design. The plasmonic metastructures were fabricated using a simplified approach to easily obtain highly reproducible nanocavity-shaped photonic crystals.[39] The plasmonic crystals which are based on a largely used copolymer (ZEP520A) and gold thin layers are realized by simple modification of a preexisting nanolithography procedure. Our novel nanostructures were fabricated by electron beam lithography (EBL). EBL is not a low-cost technique. Moreover, EBL is a fabrication technique which is technologically demanding in terms of time and expensive for a mass production destined to industrial applications. Nevertheless, it represents one of the best choices for a proof-of-concept study where in the design phase the main purpose is to test and study the physical properties of new complex nanostructures. Our main target is to design well-controlled octupolar coupling platforms using bacteriophages as recognition elements for the creation of SERS-based multifunctional biochips for rapid culture- and label-free detection of spe-

cific pathogens (*Brucella*). After the achievement of our target, the idea is scaling existing demonstrations to practical applications by its replacement with molding technique in the case of large scale production. Finally, the selected phage-based structures and the associated fabrication method can be implemented over large surfaces, which is an important prerequisite to the industrial development of plasmonic sensors.

In the frame of the "proof-of-concept phase" the first goal of our activity is to adopt a novel easy and fast fabrication technique, so as to develop highly sensitive plasmonic substrates with homogeneous density profiles for sensing based on SERS for use in food safety. To achieve such target the nanocavities configuration is designed in order to furthermore improve the plasmonic properties of a gold substrate based on an array of nano-holes. In this multilayered structure the plasmonic properties are the sum of different Surface Plasmonic Resonance (SPR) modes: propagating (Surface Plasmonic Polariton - SPP) and localized (Localized Surface Plasmon Resonance- LSPR) that in different ways contribute to the field in the different morphological region of the pattern. Furthermore, the presence of a continuous gold film allows a strong reduction of the glass substrate fluorescence, making the nanocavities configuration an ideal platform for plasmonic SERS spectroscopy.

The fabricated gold octupolar nanostructures are based on a periodic array of a meta-molecule (unit cell reported in Figure 1c) made of equilateral triangular holes in a trigonal lattice arrangement. The microscope images demonstrate the precise and very good quality production of the plasmonic nanostructures accounting for their meta-molecule shape, inter-metamolecular separation that appear uniform and regular over the pattern (see Figure 2a-b). The term "octupolar" refers to the 3-fold symmetry of the quadratic nonlinear susceptibility tensor that behaves under rotations as an octupolar charge distribution tensor.[40,41] The "fractal" structure of the nano-hole pattern is guided by the notion that increasing the number of tip-like discontinuities, that is the number of triangles and their corners over a given area, is bound to increase likewise the number of field enhancing "hot spots". Hence the choice of a central nano-hole and three surrounding ones, making altogether for 12 such corners, with the advantage in the lattice level of face-to face corners in the shape of inter-meta-molecular bow-ties known for their strong field enhancing potential. The reason to favor triangles lies in their non-centrosymmetric nature as opposed to square or circular shapes. Indeed, this is a prerequisite for quadratic nonlinear optical effects such as second-harmonic generation that we project in the longer term to combine with Raman and SERS diagnostics so as to demonstrate a multi-scheme sensor, with improved recognition and sensitivity potential. A growing number of papers report on nano-plasmonic structures with three-fold octupolar symmetry and it was our desire to build-up on this pool of nonlinear optical expertise so as to combine it with sensing requirements (see for example our reference [41] and references therein).

SERS Octupoles Performances. In order to evaluate the SERS performance of the multilayer octupolar metastructures we calculated the enhancement factor EF= $I_{SERS} \times N_{REF}/ (I_{REF} \times N_{SERS})$ using 4-MbA as molecular probe. I_{SERS} and I_{REF} are the intensities of the band at 1073 cm^{-1} and 1096 cm^{-1} in the SERS and spontaneous Raman spectrum of 4-MbA, respectively. Analogously, N_{SERS} (9×10^5) and N_{REF} (2.6×10^{11}) are the number of molecules contributing to the SERS and Raman signal, respectively. More details on the EF calculations are reported in the supporting material. Additionally, to verify the good reproducibility of the proposed SERS sensors, which is fundamental for the design of quantitatively reliable sensors for specific analytes, the amplification properties of the SERS substrates were characterized by mapping experiments performed on different samples. For each nanopattern three maps were collected covering a total area of 150 × 150 μm. For simplicity, in Figure 4 is shown only one of the three mapping experiments in which the 3D Raman images were reconstructed by considering the space-distribution of the EF over a 50×50 μm surface. To estimate the reproducibility of SERS signals over the mapped area in the same figure we reported the average spectrum (obtained from 630 spectra of the map) with its relative standard deviation.

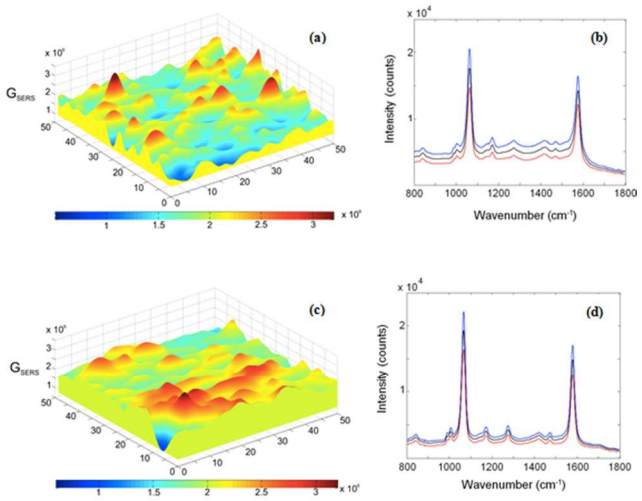

Figure 4. 3D Raman image (color map) reconstructed by considering the EF values as a function of the position in a 50 × 50 μm area of the octupolar nanostructures with A=25nm (a) and A=100nm (c). Average SERS spectrum of 4-MbA (black trace) and average SERS spectrum ± standard deviation (red and blue traces, respectively) for the nano-patterns with the two different gap distances A=25nm (c) and A=100nm (d).

For the structure with A=25nm a visual inspection of the spectra collected across the whole map (see Figure S2, Supporting Information) highlights the consistency of the SERS pattern in terms of peak frequency and shape. The average EF value, $\overline{(EF)}$, evaluated over a large number of spectra (630 of them for each map), is very good (1.8×10^6) and the homogeneity of the SERS signal is appropriate [standard deviation (std) = 16 %]. This is evidenced in the

3D Raman image (Figure 4a), by the green color of large map areas and by the relative closeness of the average spectrum with the traces relative to the average spectrum with standard deviation uncertainty (see Figure 4b).
The structure with A=100 (see Figure 4c) shows similar features to those described above, with a slightly improved $(EF)^{-}$(2.1×10^6) and a comparable response homogeneity (std = 14%) as reported in Figure 4d. As for the absolute intensity, the response is more dependent on sampling location. The results show a maximum SERS EF of ~ 2.9×10^7 and 5×10^7 for the octupolar platforms with gap A=25 nm and A= 100 nm, respectively, obtained using the QE Pro-Raman system coupled to the BX51 microscope (details are reported in the supplementary materials). Such EF values make our structure suitable for high-performances label-free SERS. Additionally, recent reports have evidenced that an enhancement factor of the order of 10^7–10^8 is sufficient for single-molecule spectroscopy.[40,41] These experimental results are confirmed by FDTD calculations as shown in Figure 2c-d. The near field distribution is dependent on the arrangement and on the shape of the units of a plasmonic structure, and on the intensity, wavelength and polarization state of the incident light.[42] The calculated total electric fields by FDTD showed that the high SERS response featured by octupolar arrays is mainly due to strongly localized electric fields at the gold–air interface of the bottom gold nanotriangles within a detection volume.

SERS Detection Performances: Bacteria Capture. In order to investigate the recognition and capture properties of the phage-based octupolar metastructure, SERS spectroscopy was used to measure the amplified Raman scattering signals from individual bacteria. SERS spectra corresponding to a single *Brucella* bacterium are shown in Figures 5a-b. Figure 5 shows both SPR and SERS response of a 4-MbA SAM (violet line), after bacteriophages immobilization (green line) and after *Brucella* bacteria capture (red line), respectively, for the two different gaps A = 25 nm and A=100nm. SERS spectra were measured from 20 randomly selected spots over the SERS substrate using the QE Pro-Raman system with a spot focus area of 1.28 μm^2. The two main peaks at 1073 cm^{-1} and 1584 cm^{-1} are mainly associated to CC stretching of the aromatic ring.
In Figure 5a the top spectrum is the SERS spectra of a single bacterium adsorbed on the multi-layer bio-sensing platform. It clearly shows that the coupling platform induces a giant enhancement of the SERS signal enabling molecular characterization of the bacteria surface down to single bacterium detection. The bottom spectrum (blue one) is taken out of the nanostructure area and does not exhibit any significant SERS signal that would have allowed to detect or to identify the immobilized phages and the captured *Brucella* bacterium. A bright field microscope image of *Brucella* bacteria captured on the top of the Au nanostructures is shown in the inset of Figure 5.
We used the area of the peak located at 1073 cm^{-1} to calculate the signal increase. An 8-fold amplification after phage immobilization and a remarkable 21-fold amplification corresponding to 107000 counts after bacteria capture were estimated. We justify these amplifications in term of local refractive index change due to the presence of immobilized phages and further on, to the captured bacteria.[39] Stable molecular interactions between phages and the 4-MbA SAM are possible based on hydrogen bonds between the carboxylic acid group of 4-MbA and the proteins of the external structure of the *Tbilisi* virus (capsid and/or fiber tails). The increase of hydrogen bonds in the system brings about a subsequent increase of the system density with a consequent variation at the nanoscale of the local refractive index. Therefore, the presence of the captured bacteria is responsible for further index variation. It is also worthwhile noting that the use of a small bacteriophage, such as *Tbilisi,* allows for a larger portion of the bacterium to be probed by the evanescent field.
In Figure 5b the SERS response of the structure is reported for a larger gap. It exhibits a significantly stronger Raman signal (134000 counts) from the virus before Brucella immobilization and a less intense signal from the captured Brucella.

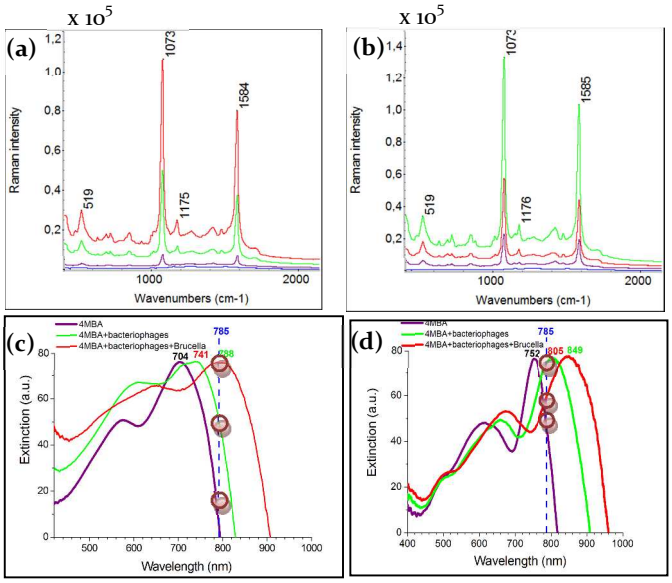

Figure 5. LSPR and SERS analysis of 4-MBA (violet line), after bacteriophagies immobilization (green line) on top of the nanostructure and after Brucella bacteria capture (red line). a-b: SERS spectra for the metastructures with interholes gaps of 25 and 100nm respectively. The SERS spectrum out of the nanostructure is sketched in blue. For these measurements we used the QE Pro-Raman system with a 10s acquisition time and 12mW laser intensity. c-d: Extinction spectra of the Au-octupolar metastructures corresponding to (a) and (b) measurements. The intersection of each curve with the excitation wavelength is highlighted with a red circle.

In order to support our previous explanation and to investigate the nature of the signal increase, we measured the extinction spectra of the meta-structures in a three steps analysis performing out-of-plane spectral transmittance measurements at normal incidence, via a standard reflection setup.[24] The variation in Raman enhancement with

the immobilized viruses and then with the captured bacteria is assigned to the variation in Surface Plasmon Resonance (SPR) position and its corresponding shift from the excitation wavelength of 785 nm. It has been reported that maximum enhancement is observed when the SPR approaches the excitation wavelength.[43-44] Figure 5 c-d shows the red-shift of the plasmonic resonance peaks for the two gaps considered. Clearly, the situation that better overlaps the region of the excitation laser wavelength (λ = 785 nm), allowing an enhancement of the resonance effect, is that represented by 4MbA+virus+*brucella* in the smaller gap structure (red line in Figure 5c). In this way, a plasmonic resonance shift associated with the gold nanopatterned structure, due to the presence of immobilized phages and to the subsequent *Brucella*'s capture, can justify a higher SERS response. Such a resonance shift is at the origin of the observed increases of the SERS signal intensity, as reported in the graph of Figure 5a. Moreover, Figure 5d shows a better match for the 4MbA+virus system when the gap is 100nm, which justifies the lower amplification of the *Brucella* signal and the more intense Raman signal coming from the system with the immobilized virus. Furthermore, at the same time we demonstrated the application of such substrate for SPR based molecular sensing. A redshift in peak wavelength from 704 to 741 nm is observed after phage immobilization (10^7 PFU/ml), and a further shift from 741 to 788 nm corresponding to *Brucella* capture (10^5 CFU/ml) for the 25 nm gap nanopattern (see Figure 5c). Likewise for the larger gap (see Figure 5d) where a red shift of 53 nm corresponds to the immobilized phages (10^7 PFU/ml) and the observation of a further 44 nm shift after *Brucella* capture (10^5 CFU/ml). In this way we could test the capacity of our sensor towards easy detection of viruses down to a 16 Femtomolar concentration. Further work is in progress to evaluate its sensitivity and detection threshold. In order to test the reproducibility of our platform the SERS response signal over different concentration of bacteria has been analyzed in the range 10^4 – 10^9 CFU/ml (see Supplementary Figs S5). Measurements have been taken testing the phage-based octupolar metastructure with gap A = 25 nm.

Specificity studies. Negative control SERS experiments were conducted to check the recognition specificity of the bound Tbilisi phages. To check the selectivity of the phage-based octupolar platform, a 300 µl (10^5 CFU/ml) bacterial suspension in water of *Escherichia Coli* was dropped on the nanostructure with gap A=25nm functionalized with bacteriophages, and maintained thereafter for 45 min. The surface was then rinsed with water and ethanol to remove non captured bacteria before SERS measurement. SERS spectra of the immobilized *Tbilisi* bacteriophages and of the *Escherichia Coli* bacteria are shown in Figure 6, indicating that the bacteria SERS signal does not exhibit any amplification compared to the phage signal. The addition of *Escherichia Coli* to the *Tbilisi* phage-based octupolar coupling system does not cause any Raman amplification. Thus, the bacterial capture experiments with the non-host control *E. coli* confirm almost negligible binding. This proves that this system is selectively sensitive to *Brucella* and not to other bacteria. To further ascertain the selectivity of the present plasmonic biosensor, the phage immobilized surfaces exposed to the host *E. coli* bacteria were also tested by optical microscopy, confirming that no capture took place after washing the samples (see inset of Figure 6).

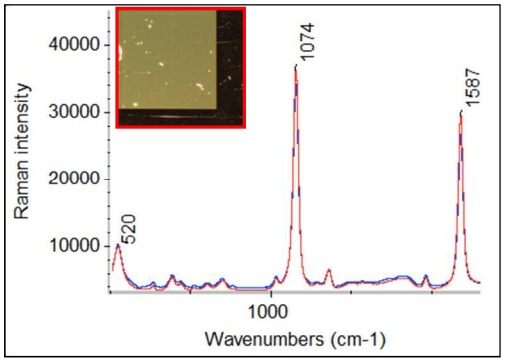

Figure 6. SERS spectra of 4-MBA after bacteriophagies immobilization (blue line) on the top of the nanostructure and after *Escherichia Coli* bacteria capture (red line). In inset dark field microscope image of captured bacteria on top of the functionalized multi-layer nanostructure.

In order to complement the evaluation of our plasmonic coupling platform, we exposed it to live *brucella* bacteria. We used here our home-made prototypal system for SERS "in situ" analysis as shown in Figure 7a. A 10 µl (10^4 CFU/ml) suspension of *Brucella* bacteria in water was dropped on the octupolar platform with gap 25nm functionalized with bacteriophages and maintained for 45 min. The surface was rinsed with water and ethanol before SERS measurement to remove non captured bacteria. SERS spectra of the immobilized *Tbilisi* bacteriophages and of the single focalized *Brucella* bacterium are shown in Figure 7b, indicating that the bacterium SERS signal exhibits a clear amplification by a 2.1 factor as compared to the phage signal. This result confirms the previous study with inactived *Brucella* where we demonstrated an amplification of 2.5.

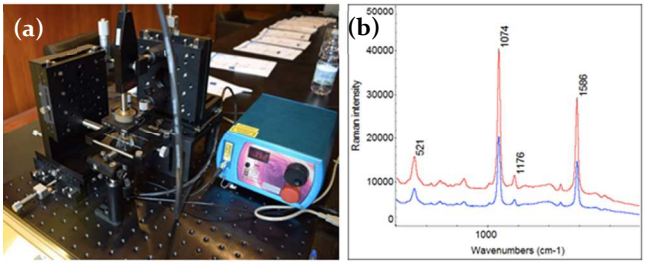

Figure 7. (a) Home-made prototypal system for SERS "in field" analysis; (b) SERS spectra of 4-MBA after bacteriophage immobilization (blue line) on the top of the nanostructure and after *Brucella* bacterium capture (red line).

CONCLUSION

In conclusion, we have conceived and demonstrated a novel large area SERS substrate made of multilayer octupolar metastructures which generate high density SERS at the triangular nanocavity sites within a detection volume. This SERS substrate shows a maximum EF of ~ $2.9x10^7$ and average EF enhancement over 106 and good uniformity (~18%). The multilayer octupolar metastructure works as a dual-functional sensing chip (SERS-SPR) with highly sensitive local refractive index detection (lower than 17 femtomolar level) and Raman enhancement. A giant enhancement of the 4-MbA SERS intensity of 107.000 counts was observed. Such performance is specifically attached to the recognition and attachment of *Brucella* bacteria in the presence of viruses. This work indicates that SERS spectroscopy in combination with innovative multi-layer octupolar metastructures properly functionalized with *Tbilisi* bacteriophages specific to *Brucella* bacteria may offer a promising alternative to detect *Brucella* as compared to agar-plates. Measurements at the single-cell level are made possible, enabling faster and more accurate identification in less than 1h while avoiding a pre-cultivation step. Our method is simple, low cost, selective and highly sensitive, opening interesting opportunities for the use of bacteriophages as recognition elements for *Brucella* detection. In the longer term, we wish to build-up on the nonlinear optical potential specific of octupolar structures and already well documented in the literature (see Ref. 39 and references therein). Such a combination could provide a multi-probing platform based on both nonlinear optical detection together with the currently demonstrated SERS-SPR probe. Such combination has the potential to provide further insights onto the polarizability and anisotropy and chirality (handedness) of the targeted specie. We also plan to employ our octupolar coupling platform towards the detection of *Brucella* within a complex environment in order to effectively move phage diagnostics from the laboratory onto the clinic. In addition, future research efforts will be aimed to immobilize different bacteriophages in order to selectively identify other clinically relevant bacterial pathogens such as *Staphylococcus Aureus*, *E. Coli*, *Salmonella* and *Listeria* at concentrations below 10^4 CFU/ml.

ASSOCIATED CONTENT

Supporting Information. Supplementary material (detailed calculation of enhancement factors and Atomic force microscopies results, Figure S1 showing Depth profile Raman measurements on a silicon wafer, Figure S2 showing SERS signals of 4-MBA spectra collected across the whole map (50×50 μm surface), Figure S3 showing SERS hot spot signals of 4-MBA spectra for the two different inter-cavities distances by the QE-Pro Raman system, Figure S4 showing AFM non-contact topography measurements, Figure S5 showing the SERS peak intensity (I_{1073}) over different concentration of bacteria) is available. This material is available free of charge via the Internet at http://pubs.acs.org.

AUTHOR INFORMATION

Corresponding Author

* Email: L.petti@isasi.cnr.it

Author Contributions

The manuscript was written through contributions of all authors. / All authors have given approval to the final version of the manuscript. / [+]These authors contributed equally.

Notes

The authors declare no competing financial interest.

ACKNOWLEDGMENT

This work was supported by the European Regional Development Fund-FESR of POR Campania 2007-2013, Call Innovation Window (Project title "Kit for Brucella Abortus e B. Melitensis nano-BIosensing Rapid detection–AMBRA"). We thank Dr. E. Bobeico from ENEA Portici Centre for her support in the fabrication process of the nanostructures.

REFERENCES

(1) Arya, S.K.; Singh, A.; Naidoo, R.; Wu, P.; McDermott , M.T.; Evoy, S. Chemically immobilized T4-bacteriophage for specific Escherichia coli detection using surface plasmon resonance. *Analyst*. **2011,** 136, 486–492.

(2) Wei, H.; Abtahi S.M.H.; Vikesland, P.J. Plasmonic colorimetric and SERS sensors for environmental analysis. *Environ. Sci.: Nano*. **2015**, 2, 120-135.

(3) Liu, T.Y.; Tsai, K.T.; Wang, H.H.; Chen, Y.; Chen, Y.H.; Chao, Y.C.; Chang, H.H.; Lin, C.H.; Wang, J.K.; Wang, Y.L. Functionalized arrays of Raman-enhancing nanoparticles for capture and culture-free analysis of bacteria in human blood. *Nat. Commun*. **2011**, 2:538, 1-8.

(4) Poltronieri, P.; Mezzolla, V.; Primiceri, E.; and Maruccio, G.. Biosensors for the Detection of Food Pathogens. *Foods* **2014**, 3, 511-526.

(5) Premasiri, W.R.; Moir, D.T.; Klempner, M.S.; Krieger, N.; Jones II, G.; Ziegler, L.D. Characterization of the Surface Enhanced Raman Scattering (SERS) of Bacteria. *J. Phys. Chem. B* **2005,** 109, 312-320.

(6) Ahijado-Guzaman, R.; Gomez-Puertas, P.; Alvarez-Puebla, R.A.; Rivas, G.; Liz-Marzan, L.M. Surface-Enhanced Raman Scattering-Based Detection of the Interactions between the Essential Cell Division FtsZ Protein and Bacterial Membrane Elements. *ACS Nano* **2012**, 6, 7514-7520.

(7) Meisel, S.; Stöckel, S.; Elschner, M.; Melzer, F.; Rösch, P.; Poppa, J. Raman Spectroscopy as a Potential Tool for Detection of Brucella spp. in Milk. *Applied and Environmental Microbiology*. **2012**, 78, 16, 5575–5583.

(8) Sonntag, M.D.; Klingsporn, J.M.; Zrimsek, A.B.; Sharma, B.; Ruvuna, L.K.; Van Duyne, R.P. Molecular plasmonics for nanoscale spectroscopy. *Chem. Soc. Rev*. **2014**, 43(4), 1230-1247.

(9) Shahbazyan, T.V.; and Stockman, M.I. *Plasmonics: Theory and Applications: Challenges and Advances in Computational Chemistry and Physics*; Springer Science, 2013.

(10) Aroca, R.F. Plasmon enhanced spectroscopy. *Phys. Chem. Chem. Phys*. **2013**, 15, 5355-5363.

(11) Tawil, N.; Sacher, E.; Mandeville, R.; Meunier, M. Bacteriophages: biosensing tools for multi-drug resistant pathogens. *Analyst* **2014**, 139, 1224-1236.

(12) Cooper, M. A.; Singleton, V. T. A Survey of the 2001 to 2005 Quartz Crystal Microbalance Biosensor Literature: Applications of Acoustic Physics to the Analysis of Biomolecular Interactions. *J. Mol. Recognit*. **2007**, 20, 154– 184.

(13) Jonsson, M. P.; Jonsson, P.; Hook, F. Simultaneous Nanoplasmonic and Quartz Crystal Microbalance Sensing: Analysis of Biomolecular Conformational Changes and Quantification of the Bound Molecular Mass. *Anal. Chem*. **2008**, 80, 7988–7995.

(14) Daniels, J. S.; Pourmand, N. Label-Free Impedance Biosensors: Opportunities and Challenges. *Electroanalysis* **2007**, 19, 1239–1257.
(15) Anker, J. N.; Hall, W. P.; Lyandres, O.; Shah, N. C.; Zhao, J.; Van Duyne, R. P. Biosensing with Plasmonic Nanosensors. *Nat. Mater*. **2008**, 7, 442–453.
(16) Nusz, G. J.; Curry, A. C.; Marinakos, S. M.; Wax, A.; Chilkoti, A. Rational Selection of Gold Nanorod Geometry for Label- Free Plasmonic Biosensors. *ACS Nano* **2009,** 3, 795–806.
(17) Homola, J. Surface Plasmon Resonance Sensors for Detection of Chemical and Biological Species. *Chem. Rev*. **2008**, 108, 462–493.
(18) Feuz, L.; Jonsson, P.; Jonsson, M.P.; Hook, F. Improving the Limit of Detection of Nanoscale Sensors by Directed Binding to High-Sensitivity Areas. *ACS Nano* **2010**, 4, 2167-2177.
(19) Cheng, I.F.; Chang, H.C.; Chen, T.Y.; Hu, C.; Yang, F.L. Rapid (<5 min) Identification of Pathogen in Human Blood by Electrokinetic Concentration and Surface-Enhanced Raman Spectroscopy. *Scientific Reports*, **2013**, 3, 2365.
(20)Harper, M.M.; McKeating, K.S.; Faulds, K. Recent developments and future directions in SERS for bioanalysis. *Phys Chem Chem Phys*., **2013**, 15, 5312-5328.
(21) Petti, L.; Capasso, R.; Rippa, M., Pannico, M.; La Manna, P.; Peluso, G.; Calarco, A.; Bobeico, E.; and Musto, P. A Plasmonic Nanostructure Fabricated by Electron Beam Lithography as a Sensitive and Highly Homogeneous SERS Substrate for Biosensing Applications. *Vibrational Spectroscopy*. **2016**, 82, 22–30.
(22) Oh, Y.J.; Jeong, K.H. Glass Nanopillar Arrays with Nanogap-Rich Silver Nanoislands for Highly Intense Surface Enhanced Raman Scattering. *Adv. Mater*. **2012**, 24, 2234–2237.
(23) Wang, Y.; Lu, N.; Wang, W.; Lu, L.; Feng, L.; Zeng, Z.; Li, H.; Xu, W.; Lu, Y.; Chi, L. Highly effective and reproducible surface-enhanced Raman scattering substrates based on Ag pyramidal arrays. *Nano Research* **2013**, 6(3), 159–166.
(24) Chen, D.; Zhou, J.; Rippa, M.; Petti., L. Structure-dependent LSPR Characteristics and SERS Performances of Quasi-periodic Nano-arrays: Measurements and Analysis. *Journal of Applied Physics*, **2015** 118, 163101 .
(25) Lei Shu, Y.; Zhou, J.; Yuan, X.; Petti, L.; Chen, J.; Jia, Z.; Mormile, P. Highly Sensitive Immunoassay Based on SERS Using Nano-Au Immune Probes and a Nano-Ag Immune Substrate. *Talanta*, **2014** 123, 161–168.
(26) Ma, Y.; Zhou, J.; Zou,W.; Jia, Z.; Petti, L.; Mormile, P. Localized surface plasmon resonance and surface enhanced Raman scattering responses of Au@Ag core-shell nanorods with different thickness of Ag shell. *Journal of Nanoscience and Nanotechnology*, **2014**, 14 (6), 4245-4250.
(27) Etchegoin, P. G.; Le Ru, E. C. A perspective on single molecule SERS: Current status and future challenges. *Phys. Chem. Chem. Phys.* **2008**, 10, 6079–6089.
(28) Le Ru, E. C.; Blakie, E.; Meyer, M.; Etchegoin, P. G. Surface enhanced Raman scattering enhancement factors: A comprehensive study. *J. Phys. Chem. C*. **2007**, 111, 13794–13803.
(29) Petti, L.; Capasso, R.; Rippa, M.; Zhou, J.; Maglione, M.G.; Pannico, M.; La Manna, P.; Musto, P. Plasmonic Octagonal Quasi Crystals for Surface-Enhanced Raman Sensing. Advanced Device Materials, **2015**. 1, 2.
(30) Van der Merwe, R.G.; van Helde, P.D.; Warren, R.M.; Sampson, S.L.; and Gey van Pittius, N.C. Phage-based detection of bacterial pathogens. *Analyst,* **2014**, 139, 2617-2626.
(31) Singh, A.; Arutyunov, D.; McDermott, M.T.; Szymanskic, C.M.; Evoy, S. Specific detection of Campylobacter using the bacteriophage NCTC 12673 receptor binding protein as a probe. *Analyst,* **2011**, 136, 4780–4786.
(32) Tawil, N.; Sacher, E.; Mandeville, R.; and Meunier, M. Surface plasmon resonance detection of E.coli and methicillin-resistant S. aureus using bacteriophages. *Biosensors and Bioelectronics*, **2012**, 37, 24-29.
(33) Singh, A.; Glass, N.; Tolba, M.; Griffiths, M.; and Evoy, S. Immobilization of bacteriophages on gold surfaces for the specific capture of pathogens. *Biosensors and Bioelectronics*, **2009**, 24 3645–3651.
(34) Balasubramanian, S.; Sorokulova, I.B.,;Vodyanoy, VJ; Simonian, AL. Lytic phage as a specific and selective probe for detection of Staphylococcus aureus--A surface plasmon resonance spectroscopic study. *Biosens Bioelectron*. **2007**, 22(6), 948-55.
(35) Nanduri, V., Sorokulova, I.B., Samoylov, A.M., Simonian, A.L., Petrenko, V.A., Vodyanoy, V. Phage as a molecular recognition element in biosensors immobilized by physical adsorption. *Biosens. Bioelectron*. **2007,** 22 (6), 986–992.
(36) Sambrook, J.; Russell, D.W. *Molecular Cloning: A Laboratory Manual*; CSHL Press, 2001.
(37) Wang, Y., Ji, W., Sui,H., Kitahama, H., Ruan, W., Ozaki,Y., Zhao,B. Exploring the Effect of Intermolecular H-Bonding: A Study on Charge-Transfer Contribution to Surface-Enhanced Raman Scattering of p-Mercaptobenzoic Acid. *J. Phys. Chem.* **2014**, 118 (19), 10191–10197.
(38) Wang, F., Widejko, R. G., Yang, Z., Nguyen, K. T., Chen, H., Fernando, L. P., Christensen, K. A., Anker, J. N. Surface-enhanced raman scattering detection of pH with silica-encapsulated 4-mercaptobenzoic acid-functionalized silver nanoparticles. *Anal. Chem*. **2012**, 84, 8013–8019.
(39) Rippa, M.; Castagna, R.; Pannico, M.; Musto, P.; Bobeico, E.; Zhou, J.; Petti, L. High-performance Nanocavities-based Metacrystals for Enhanced Plasmonic Sensing. *Optical Data Processing and Storage* **2016**, 2 (1), 22-29.
(40) Zyss, J. Molecular Engineering Implications of Rotational Invariance in Quadratic Nonlinear Optics: From Dipolar to Octupolar Molecules and Materials. *J. Chem. Phys*. **1993**, 98, 6583–6599.
(41) Kolkowski, R.; Petti, L.; Rippa, M.; Lafargue, C.; Zyss, J. Octupolar Plasmonic Meta-Molecules for Nonlinear Chiral Watermarking at Subwavelength Scale. *ACS Photonics*, **2015**, 2(7), 899-906.
(42) Yu, Q.; Braswell,S.; Christin, B.; Xu, J.; Wallace, P.M.; Gong, H.; Kaminsky, D. Surface-enhanced Raman scattering on gold quasi-3D nanostructure and 2D nanohole arrays. *Nanotechnology* **2010**, 21, 355301-10.
(43) Garcia, M. A. Surface plasmons in metallic nanoparticles: Fundamentals and applications. *J. Phys. D: Appl. Phys*. **2011**, 44, 283001.
(44) Haynes, C.L.; Yonzon, C.R.; Zhang, X.; Van Duyne, R.P. Surface-enhanced Raman sensors: early history and the development of sensors for quantitative biowarfare agent and glucose detection. *J. Raman Spectrosc*. **2005**, 36, 471–484.

SYNOPSIS TOC